Journal of Cerebral Blood Flow & Metabolism (2013) 33, 263–271

www.jcbfm.com

ORIGINAL ARTICLE

Oxygen consumption rates during three different neuronal activity states in the hippocampal CA3 network

Christine Huchzermeyer[1,5], Nikolaus Berndt[2,5], Hermann-Georg Holzhütter[2,6] and Oliver Kann[3,4,6]

The brain is an organ with high metabolic rate. However, little is known about energy utilization during different activity states of neuronal networks. We addressed this issue in area CA3 of hippocampal slice cultures under well-defined recording conditions using a 20% O_2 gas mixture. We combined recordings of local field potential and interstitial partial oxygen pressure (pO_2) during three different activity states, namely fast network oscillations in the gamma-frequency band (30 to 100 Hz), spontaneous network activity and absence of spiking (action potentials). Oxygen consumption rates were determined by pO_2 depth profiles with high spatial resolution and a mathematical model that considers convective transport, diffusion, and activity-dependent consumption of oxygen. We show that: (1) Relative oxygen consumption rate during cholinergic gamma oscillations was 2.2-fold and 5.3-fold higher compared with spontaneous activity and absence of spiking, respectively. (2) Gamma oscillations were associated with a similar large decrease in pO_2 as observed previously with a 95% O_2 gas mixture. (3) Sufficient oxygenation during fast network oscillations *in vivo* is ensured by the calculated critical radius of 30 to 40 μm around a capillary. We conclude that the structural and biophysical features of brain tissue permit variations in local oxygen consumption by a factor of about five.

Journal of Cerebral Blood Flow & Metabolism (2013) **33,** 263–271; doi:10.1038/jcbfm.2012.165; published online 21 November 2012

Keywords: brain slice; capillaries; electrophysiology; energy metabolism; mathematical modeling; mitochondria

INTRODUCTION

The brain receives ~15% of the cardiac output and is especially sensitive to hypoxia, which suggests that neuronal activity is associated with high energetic costs and requires intact function of mitochondria.[1] Although the total oxygen consumption of the brain is almost constant, large local variations might occur during different activity states in the respective brain region.[2–4] Local changes in oxygen consumption *in vivo* are commonly inferred from the slope of the decrease in the interstitial partial oxygen pressure (pO_2) recorded during stop of oxygen supply or activation of specific brain regions. However, such measurements are strongly influenced by adaptations of the cerebral blood flow accompanying any perturbation of oxygen homeostasis.[5–7] Because of this compensatory hemodynamic response, data on activity-dependent oxygen consumption in certain brain regions or even in small neuronal networks by functional magnetic resonance imaging (blood oxygen level-dependent signal) or tissue oxygenation measurements *in vivo* are difficult to interpret and might misjudge real changes in cerebral oxygen consumption.[4,8] For these reasons, brain slice preparations *in vitro*, in which hemodynamic responses are absent, may be an useful model to quantify the oxygen consumption rates during different activity states.[9–11] Slice preparations permit recordings of pO_2 and the local field potential (LFP) with microelectrodes. In addition, recordings are performed under well-defined conditions such as constant oxygen supply and experimental induction of specific activity states in a given neuronal network.[11–13]

In the present study, we determined oxygen consumption rates during three different activity states in hippocampal area CA3 by using slice cultures. As a high activity state, we induced fast neuronal network oscillations in the gamma-frequency band (30 to 100 Hz) by application of acetylcholine, which mimics cholinergic input from the septum *in vivo*.[12,14] Gamma oscillations have been implicated in several higher cognitive functions, such as sensory processing, memory formation, and attentional selection.[14,15] The two other activity states were spontaneous network activity, which occurs in hippocampal slice cultures despite the lack of (sub)cortical input,[13,16] and the absence of action potentials (spiking) in the network that was induced by application of tetrodotoxin (TTX). To be able to perform the experiments under more physiologic conditions, i.e., applying a 20% O_2 gas mixture, we used hippocampal slice cultures on an intact Biopore membrane in a modified interface recording chamber. During the three activity states, we determined pO_2 profiles in slice cultures with high spatial resolution. For detailed analysis of the pO_2 profiles, we used a mathematical reaction-diffusion model to quantify the contribution of oxygen transport and activity-dependent oxygen consumption rates.

[1]Institute for Neurophysiology, Charité-Universitätsmedizin Berlin, Berlin, Germany; [2]Institute of Biochemistry, Charité-Universitätsmedizin Berlin, Berlin, Germany; [3]Institute of Physiology and Pathophysiology, University of Heidelberg, Heidelberg, Germany and [4]Interdisciplinary Center for Neurosciences (IZN), University of Heidelberg, Heidelberg, Germany. Correspondence: Dr H-G Holzhütter, Division of Computational Systems Biochemistry, Institute of Biochemistry, Charité-Universitätsmedizin Berlin, Reinickendorfer Strasse 61, D-13347 Berlin, Germany or Dr O Kann, Division of General Neurophysiology, Institute of Physiology and Pathophysiology, University of Heidelberg, Im Neuenheimer Feld 326, D-69120 Heidelberg, Germany.
E-mail: hergo@charite.de or oliver.kann@physiologie.uni-heidelberg.de
This work was supported by Deutsche Forschungsgemeinschaft in SFB-618.
[5]These authors contributed equally to this work.
[6]These authors contributed equally to this work.
Received 5 June 2012; revised 5 September 2012; accepted 15 October 2012; published online 21 November 2012

MATERIALS AND METHODS

Organotypic Hippocampal Slice Cultures and Recording Chamber

Animals were housed, cared, and killed in accordance with the recommendations of the European Commission and the Berlin Animal Ethics Committee (LAGeSo, T0032/08). Organotypic hippocampal slice cultures were prepared as described.[13,17] In brief, hippocampal slices (400 μm) were cut with a McIlwain tissue chopper (Mickle Laboratory Engineering Company Ltd., Guildford, UK) from 7- to 9-day-old Wistar rats under sterile conditions. Slices were maintained on Biopore membranes (Millicell standing inserts; Millipore, Eschborn, Germany) between culture medium (50% minimal essential medium, 25% Hank's balanced salt solution (Sigma, Taufkirchen, Germany), 25% horse serum (Invitrogen, Life Technologies GmbH, Darmstadt, Germany), and 2 mmol/L L-glutamine at pH 7.3) and humidified normal atmosphere (5% CO_2, 36.5°C) in an incubator (Unitherm 150, UniEquip, Martinsried, Germany). Biopore membranes provide high viability and excellent trans-membrane oxygen transport. The culture medium (1 mL) was replaced three times per week. Slice cultures were used after 5 to 9 days *in vitro* (residual thickness of 331 ± 6 μm, $n = 29$), when the tissue had recovered from the slice preparation and damaged cut surfaces were reorganized.[10]

By contrast to recent reports, in which pieces of Biopore membrane carrying slice cultures had been cut out,[13,17] recordings were made in a modified, custom-built recording chamber (workshop in Dr Uwe Heinemann's Laboratory, Institute for Neurophysiology, Charité-Universitätsmedizin Berlin and workshop in the Institute of Physiology and Pathophysiology, University of Heidelberg) that allows the usage of intact Biopore membrane inserts (Figure 1). With this modification, slice cultures were strictly retained in the so-called interface recording condition, i.e., maintaining the slice culture at the interface between recording solution and ambient gas mixture. Intact Biopore membrane inserts ensure constant supply of oxygen and glucose from the recording solution (rate 2 mL/min) that flows underneath the membrane carrying slice cultures; the interface condition allows constant oxygen supply from the ambient gas mixture. With this approach, gassing the recording chamber with a mixture of 20% O_2, 75% N_2, and 5% CO_2 (rate 1.5 L/min) was sufficient to induce persistent gamma oscillations.

Solutions and Recordings

Slice cultures were constantly supplied with prewarmed (34 ± 1°C) recording solution (artificial cerebrospinal fluid) that contained: 129 mmol/L NaCl, 3 mmol/L KCl, 1.25 mmol/L NaH_2PO_4, 1.8 mmol/L $MgSO_4$, 1.6 mmol/L $CaCl_2$, 26 mmol/L $NaHCO_3$, and 10 mmol/L glucose. The pH was 7.3, when the recording solution was saturated with the gas mixture (20% O_2, 75% N_2, 5% CO_2). Gamma oscillations were induced by bath application of cholinergic receptor agonist, acetylcholine and acetylcholine-esterase inhibitor, physostigmine.[13] The absence of action potentials (spiking) was induced by bath application of TTX, which blocks fast voltage-gated Na^+ channels. Acetylcholine was from Sigma-Aldrich (Taufkirchen, Germany), and physostigmine and TTX were from Tocris (Biotrend, Köln, Germany).

The LFPs were recorded in *stratum pyramidale* of area CA3 with glass electrodes filled with recording solution. Changes in voltage were digitized at 10 kHz (low-pass filter of 3 kHz; CED 1401 interface; Cambridge Electronic Design, Cambridge, UK). The pO_2 was measured at different depths of the CA3 area by using oxygen sensor microelectrodes (O_2 sensors), standard OX10 (Unisense, Aarhus, Denmark). This new type of modified polarographic Clark electrode consists of a glass-insulated Ag/AgCl reference anode and a guard cathode with the advantages of low sensitivity to motion artifact, minimal interaction with tissue, and low O_2 consumption; it has been successfully used *in vitro* and *in vivo*.[13,18,19] The standard OX10 has a tip diameter of 8 to 12 μm and a spatial resolution of 1 to 2 times the outside tip diameter; further details are given in manufacturer's homepage (http://www.unisense.com). The drift of the O_2 sensors in our set-up was < 2 mm Hg/20 min.[17] The O_2 sensor was connected to a polarographic amplifier (Chemical Microsensor II; Diamond General Development, AnnArbor, MI, USA) and polarized with -0.8 V overnight. For recordings, the O_2 sensor was fixed in a mechanical micromanipulator in an angle of 55° and moved forward in steps of 20 μm

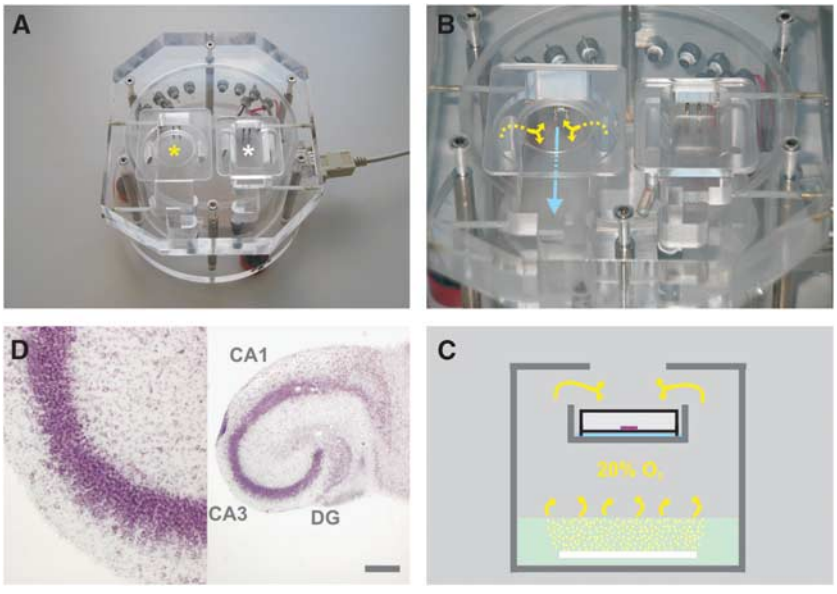

Figure 1. Illustration of recording conditions and organotypic hippocampal slice cultures. (**A**) The custom-built acrylic glass unit contains two recording chambers that are used for maintenance of slice cultures on intact Biopore membrane inserts (left chamber, yellow asterisk) or acute brain slices (right chamber, white asterisk). (**B**) The recording solution (blue arrow) is supplied by an external peristaltic pump (not shown); the gas mixture (yellow arrows) is constantly exchanged. (**C**) The simplified scheme illustrates the functional design of the unit. The bottom part contains distilled water (mint rectangle) that is permanently warmed to 34 ± 1°C. The gas mixture (20% O_2) is bubbled into the distilled water via a looped perforated plastic tube (white bar) for warming and humidification and guided (yellow arrows) to the intermediate floor. On the intermediate floor, the warmed and gas-saturated recording solution (blue bar) flows underneath the intact Biopore membrane insert (white rectangle with black lines; open from above) carrying slice cultures (purple bar). For recordings of local field potential (LFP) and partial oxygen pressure (pO_2), microelectrodes are positioned in slice cultures, through an opening in the cover plate and by using micromanipulators (not shown). (**D**) Morphologic characteristics of organotypic hippocampal slice cultures. The slice was maintained in culture for 12 days, then fixed, sectioned, and stained with cresyl violet. Note the 'organotypic' preservation of hippocampal areas, CA1, CA3, and dentate gyrus (DG), including cell layers and functional connections (right image). Recordings of LFP and pO_2 depth profiles were conducted in *stratum pyramidale* in area CA3 (purple cell layer, left image). The scale bar denotes 500 μm.

(corresponding to a vertical depth of 16 μm per step). Before and after each experiment, O_2 sensors were individually calibrated.[13] Changes in voltage were low-pass filtered and digitized at 1 kHz (CED 1401). Converted data (LFPs and pO_2) were recorded with a personal computer using Spike2 software (CED).

Cresyl Violet Staining

Slice cultures were fixed in paraformaldehyde (4%, 0.1 mol/L phosphate buffer; Sigma-Aldrich) and, thereafter, incubated with sucrose solution (30%, 0.15 mol/L phosphate buffer; Sigma-Aldrich) for 12 hours. Thin slice sections (30 μm) were cut with a freezing microtome (Leica Microsystems, Wetzlar, Germany). Sections were exposed to an ethanol series (6 steps, 3 minutes each) and rinsed in distilled water. Sections were immersed in cresyl violet solution (0.5% cresyl violet in distilled water; Sigma-Aldrich) for 90 seconds, rinsed in distilled water, and transferred to differentiation solution (200 mL, 50% ethanol, 3 drops of acetic acid). Subsequently, sections were exposed to a series of ethanol (4 steps, 3 minutes each), 2-propanol (two times; Sigma-Aldrich), and xylol (two times; Sigma-Aldrich) and finally embedded with DePeX (Serva Electrophoresis GmbH, Heidelberg, Germany).

Data Analysis

Power spectra were calculated from data segments of 60 seconds with Spike2 software (CED), using Hanning window and a bin resolution of 3.052 Hz. Data are presented as mean ± standard error and were derived from a total of 29 organotypic hippocampal slice cultures, from at least three rats per experimental group. Statistical significance ($P<0.05$) was determined by applying one-way ANOVA with Bonferroni's *post hoc* test comparing multiple groups with normal distribution. Statistical analysis and figures were made using Origin (Microcal Software, Northampton, MA, USA), SPSS for Windows (Version 19, SPSS Inc., Chicago, IL, USA) and CorelDRAW (Corel Corporation, Ottawa, Ontario, Canada).

Mathematical Reaction-Diffusion Model

The recorded pO_2 profiles were reproduced by a mathematical model that takes into account oxygen transport through neuronal tissue and activity-dependent oxygen consumption rates. We subdivided the space of the slice in N layers, of 1 μm thickness ($\Delta x = 1\ \mu m$). Within a single layer, oxygen level and oxygen consumption rate were assumed to be constant. The time-dependent change of pO_2 in layer i,

$$\frac{d(pO_2^i)}{dt} = I^i_{influx} - v^i_{consumption} - I^i_{efflux} \quad (1)$$

is the sum of three components: influx from preceding layer ($i-1$), consumption within the layer, and efflux to the following layer ($i+1$), whereby index I labels the layers from the slice surface ($i=1$) to the slice core ($i=N$). For the oxygen consumption term, we assumed Michaelis-Menten type kinetics:[20]

$$v^i_{consumption} = A\frac{pO_2^i}{pO_2^i + K_m} \quad (2)$$

The constant A is given by the cell density of the layer and the average activity of neurons and glial cells. The numerical value of K_m was put to 3 mm Hg.[19] We assume A to be constant throughout each individual slice and K_m to be constant for all slices. For A, this is certainly an abstraction from the 'real' situation because local variations in oxygen consumption are likely present due to the spatial arrangements of dendrites, soma and axons as well as different activity states. It is, however, not possible for us to make feasible assumptions for such variations. However, the value of K_m represents enzymatic properties of the respiratory chain; thus, a high variability in each slice is unlikely. The precise value of K_m is less important as long as the tissue pO_2 is much larger than K_m, which is the case in (almost) all conditions.

Since all measured pO_2 profiles show convex behavior (see below), we modeled the influx term as the sum of two components. One component is oxygen diffusion described by Fick's law:

$$I^i_{influx-diff} = D\times\frac{(pO_2^{i-1} - pO_2^i)/\Delta x^i}{\Delta x^i} \quad (3)$$

where D is the diffusion coefficient. For D, we took the value of $1.6\times10^3\ \mu m^2/s$ as reported for neuronal tissues.[21–23] The other component is a convective oxygen transport between layer i and $i+1$:

$$I^i_{influx-c} = B^i_c\times\frac{(pO_2^{i-1} - pO_2^i)/\Delta x^i}{\Delta x^i} \quad (4)$$

Adjustment of the model to measured pO_2 profiles showed that B^i_c can be well approximated by an exponential decay function:

$$B^i_c = B_0\ \exp(-\lambda/x^i) \quad (5)$$

where λ is the decay length and x^i denotes the distance of the i-th layer from the upper surface. The pressure parameter B_0 is given by the experimental set-up and was held at the same constant value for all simulated pO_2 profiles. At stationary conditions, mass balance requires efflux from layer i to be equal to influx into layer ($i+1$):

$$I^i_{efflux} = I^{i+1}_{influx} \quad (6)$$

Equation (1) must be completed by boundary conditions. The model was fitted to the part of pO_2 profile recorded between the upper surface and the pO_2 minimum, obeying well-defined boundary conditions. Since the oxygen concentration is kept constant at the upper surface of the slice culture through continuous oxygenation it holds the Neumann boundary condition:

$$pO_2^1 = const. \quad (7)$$

In the layer (i_0) where pO_2 reaches its minimum the oxygen efflux must be zero (Dirichlet boundary condition):

$$I^{i0}_{efflux} = 0 \quad (8)$$

For each slice culture, the two parameters A and λ were determined by least-square fitting of the model to the corresponding experimental pO_2 profile.

RESULTS

Three Different Activity States of the Hippocampal CA3 Network

The neuronal network was spontaneously active in *stratum pyramidale* of area CA3 in organotypic hippocampal slice cultures (Figure 2; SPON, $n=19$). Spontaneous activity was of variable degree, perhaps because of the lack of afferent inputs as well as individual differences in rhythm generators and connectivity.[13,16] Bath application of TTX (1 μmol/L) led to complete suppression of neuronal spiking and thus spontaneous network activity after ~20 minutes (Figure 2; TTX, $n=8$). Bath application of acetylcholine (2 μmol/L) and physostigmine (400 nmol/L) resulted in persistent gamma oscillations after ~30 minutes (Figure 2; GAM). The mean peak frequency of gamma oscillations was 48.7 ± 2.9 Hz ($n=8$). In contrast to earlier studies,[11,13] the induction of gamma oscillations in a 20% O_2 gas mixture was possible because of improved recording conditions (Materials and methods). A detailed analysis of cholinergically induced gamma oscillations in hippocampal slice cultures and acute slices from rat and mouse was published recently.[17] Notably, our experiments in slice cultures were conducted in the absence of any anesthetics that significantly interfere with both neuronal activity and energy metabolism.[24,25]

Depth Profiles of pO_2 During the Activity States

By using oxygen sensor microelectrodes that have been successfully used *in vitro* and *in vivo*,[13,18,19] we recorded depth profiles of pO_2 with vertical steps of 16 μm. Thus, we were able to determine the pO_2 in virtually any neuronal cell layer (z axis) of a given slice culture,[26] and with much higher spatial resolution as reported previously.[17,27,28] The lowest pO_2 values were found below the slice core, indicating a better oxygen supply from the upper slice surface (exposed to ambient gas mixture) compared with the lower slice surface (exposed to recording solution) (Figure 3A). Lowest pO_2 values differed significantly when comparing the three activity states (TTX, 90 ± 9 mm Hg; SPON, 47 ± 6 mm Hg; GAM, 18 ± 3 mm Hg; $P\leqslant0.01$) (Figure 3B). Notably, during gamma oscillations the pO_2 never decreased down to 0 mm Hg; the lowest value of 5 mm Hg was determined 16 μm below the slice core in a slice culture of 361 μm thickness.

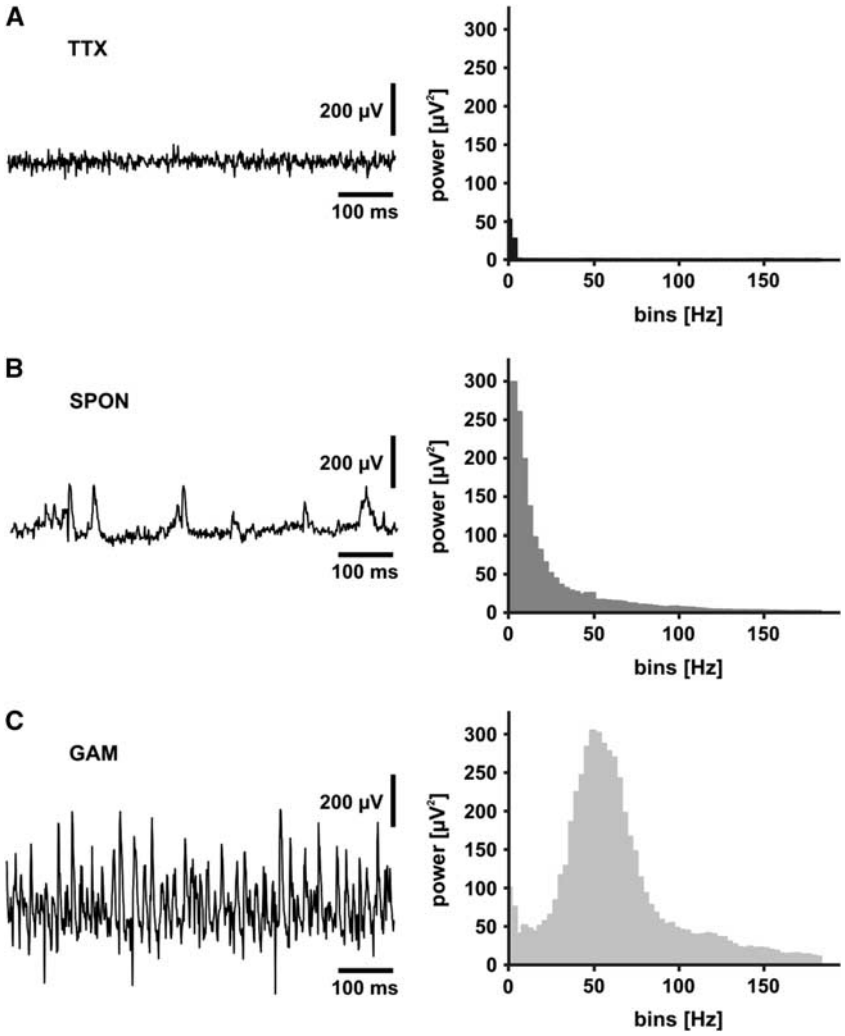

Figure 2. Three different activity states of the hippocampal CA3 network. Recordings of the local field potential (LFP) were conducted in *stratum pyramidale* of area CA3 in organotypic hippocampal slice cultures. (**A**) Bath application of tetrodotoxin (TTX) (1 μmol/L) resulted in the complete absence of spiking after $\sim$20 minutes (TTX, $n = 8$); compare with (**B**). (**B**) Spontaneous network activity (SPON, $n = 19$) was present to a variable degree in all slice cultures investigated. (**C**) Bath application of cholinergic receptor agonist, acetylcholine (2 μmol/L) and acetylcholine-esterase inhibitor, physostigmine (400 nmol/L) resulted in persistent gamma oscillations after $\sim$30 minutes (GAM, $n = 8$). The corresponding power spectra were calculated from data segments of 60 seconds (TTX, black; SPON, dark gray, GAM, light gray). Note the presence of gamma oscillations with a peak frequency of $\sim$50 Hz (lower power spectrum). A detailed analysis of cholinergically induced gamma oscillations in rat hippocampal slice cultures was published recently.[17]

For further detailed analysis, we included pO_2 values from five defined depth levels of each slice culture in the evaluation: at the upper slice surface (depth level 1), in the middle of upper surface and slice core (depth level 2), in the slice core (depth level 3), in the middle of slice core and lower slice surface (depth level 4), and at the lower slice surface (depth level 5) (Figures 3A and 3C). Compared with spontaneous network activity, gamma oscillations were associated with significantly larger decreases in pO_2 in depth levels 2 and 3. Compared with the absence of spiking (TTX), spontaneous network activity (SPON), and gamma oscillations (GAM) were associated with significantly larger decreases in pO_2 in all depth levels below the upper slice surface ($P < 0.01$). Notably, gamma oscillations that were induced under improved recording conditions and using a 20% O_2 gas mixture (Materials and methods) were associated with large decreases in pO_2, similar to those obtained with a 95% O_2 gas mixture in both hippocampal slice cultures and acute slices from rat and mouse.[17]

Quantification of Oxygen Consumption Rates

To quantify the oxygen consumption rates during the three activity states in the CA3 network, we used a mathematical reaction-diffusion model (Materials and methods). We fitted all pO_2 profiles separately to the model described above. Fit parameters were the decay length λ and the oxygen consumption rate A for each slice culture as well as the pressure component B_0 for all slice cultures that was given by the experimental settings rather than being a property of biologic material. This was performed for five different values of D. The optimal value for B_0 was $40 \times D$. The goodness of fits achieved with the model can be appreciated from three representative pO_2 profiles that are given in Figures 4A to 4C. Mean r^2 values did not differ between the groups (TTX, 0.982 ± 0.009; SPON, 0.987 ± 0.003; GAM, 0.998 ± 0.001; $P > 0.2$). All pO_2 profiles and respective fits are provided in Supplementary Figures S1 to S4. Inspection of the obtained model parameters showed that the contribution of convective oxygen transport dominates over diffusion in the

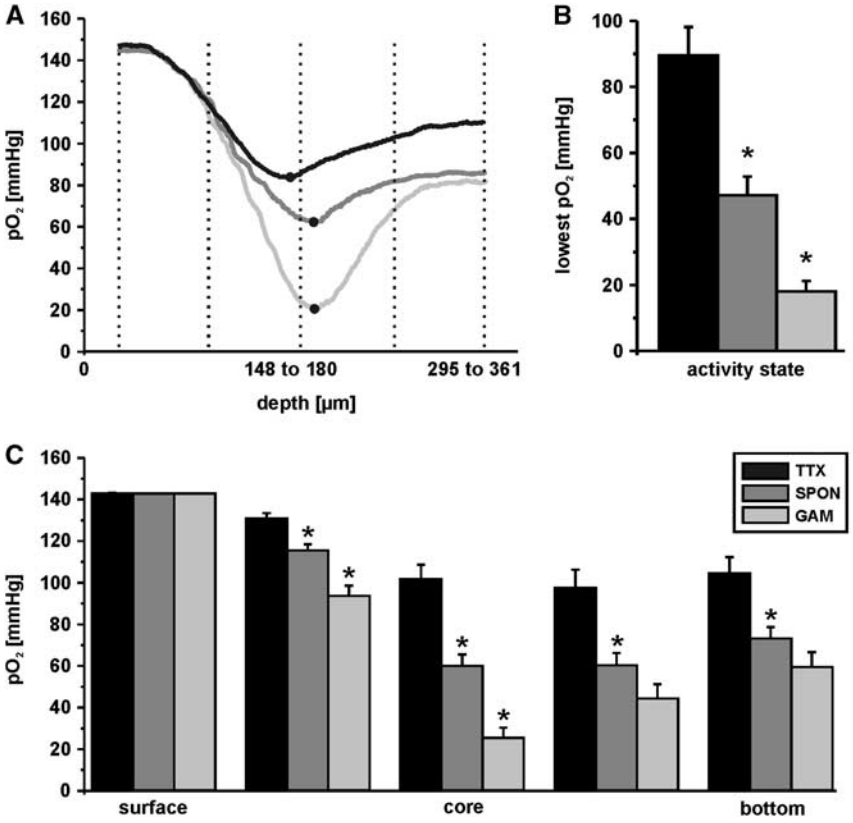

Figure 3. Depth profiles of partial oxygen pressure (pO_2) during the three different activity states. The activity states of the hippocampal CA3 network (Figure 2) were verified in each individual slice culture and pO_2 depth profiles were recorded with vertical steps of 16 μm. (**A**) Representative sample traces of pO_2 depth profiles in the absence of spiking (TTX, black trace), spontaneous network activity (SPON, dark gray trace), and cholinergically induced gamma oscillations (GAM, light gray trace). Tetrodotoxin (TTX, 1 μmol/L) as well as acetylcholine (2 μmol/L) and physostigmine (400 nmol/L) for induction of gamma oscillations were applied with the recording solution. (**B**) Quantification of lowest pO_2 values as determined during the three different activity states, i.e., TTX ($n = 8$), SPON ($n = 19$), and GAM ($n = 8$). Lowest pO_2 values are indicated by black dots in the example traces (**A**). (**C**) Quantification of pO_2 values at five defined depths in slice cultures, i.e., at the upper slice surface (surface; depth level 1), in the middle of upper surface and slice core (depth level 2), in the slice core (core; depth level 3), in the middle of slice core and lower slice surface (depth level 4), and at the lower slice surface (bottom, depth level 5) for TTX ($n = 8$), SPON ($n = 19$), and GAM ($n = 8$). Statistical significance is marked by asterisks ($P < 0.05$).

upper layers of slice cultures where the experimentally determined pO_2 profile has a convex shape (see below). This is due to construction and gas exchange in the interface chamber (Figure 1).

The comparison of mean values that were obtained during the three activity states in the CA3 network revealed a positive correlation between oxygen consumption and degree of activity in slice cultures (Figure 4D). Importantly, relative oxygen consumption rate during gamma oscillations (GAM) was 2.2-fold higher than during spontaneous network activity (SPON, $P = 0.003$) and 5.3-fold higher than in the absence of spiking (TTX, $P < 0.001$). Comparison of the averaged values of TTX and SPON showed a clear trend. However, both values did not differ significantly ($P = 0.51$). Using a value of 1.6×10^3 $\mu m^2/s$ for D in the calculation, absolute values of oxygen consumption rates (A) for the three conditions were $\sim$2.1 mmol/L per minute (TTX), 4.6 mmol/L per minute (SPON), and 11 mmol/L per minute (GAM). These values are higher than calculated for hippocampal acute slices,[29] which might be primarily due to experimental settings and the (evoked) activity state in the slices;[17] they are closer to values estimated for the gray matter of the conscious albino rat.[30] Different values of D changed the fit values for A in an equivalent manner but left the relative consumption rates unchanged (Table 1).

Implications for Oxygenation of Neuronal Tissue *In Vivo*

According to our results from mathematical modeling, the contribution of convective oxygen transport dominates over diffusion. The central role of this convective component for sufficient oxygen supply into the depth of the slice is illustrated in Figure 5, where the convective contribution was put to zero. The resulting pO_2 profiles reveal that during both spontaneous network activity and gamma oscillations the tissue oxygenation decreases to zero in a distance of $<$100 and 70 μm, respectively. This finding corresponds to our experimental observation that switching off the gas supply to the interface recording chamber and only retaining the gassing of the recording solution resulted in macroscopic swelling of the slice and necrosis of the neurons. Under these conditions, it was not possible to achieve a steady-state pO_2 profile.

To apply the model to the *in vivo* situation, in which oxygen from capillaries reaches the brain parenchyma only by diffusion, we again neglected the convective oxygen transport in our model and put the pO_2 in the capillary to 55 and 28 mm Hg. These values have been reported under physiologic conditions *in vivo*.[7,19,31] These simulations reveal that during both spontaneous network activity and gamma oscillations sufficient oxygenation of the brain parenchyma is only ensured in a radius of $\sim$30 to 60 μm (Figures 5B and 5C). The simulations also show that a vascular pO_2

of 40 mm Hg would still ensure maintenance of gamma oscillations in a radius of $\sim 35\,\mu$m around capillaries (Figure 5C). Intriguingly, this critical radius is in line with reported distances of 30 to 40 μm between capillaries in the brain.[31,32] Lower oxygen boundary conditions would require a hemodynamic response to maintain gamma oscillations.[7]

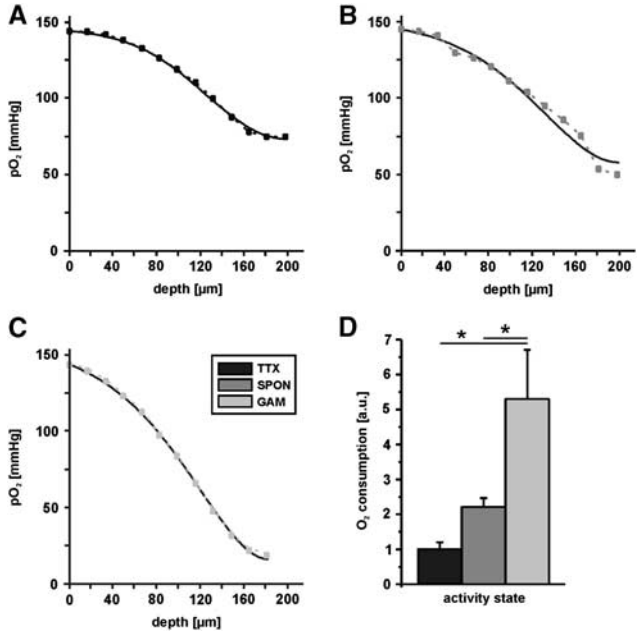

Figure 4. Fittings of partial oxygen pressure (pO_2) depth profiles and calculation of oxygen consumption. Fittings (black lines) of representative pO_2 depth profiles during the three different activity states of the hippocampal CA3 network, i.e., tetrodotoxin (TTX) (**A**), spontaneous network activity (SPON) (**B**), and gamma oscillations (GAM) (**C**) as obtained from experiments illustrated in Figure 3. Note that pO_2 depth profiles show a convex behavior. The data were fitted from the upper slice surface to the lowest pO_2 value. (**D**) Quantification of oxygen consumption in the absence of spiking (TTX, $n = 8$), during spontaneous network activity (SPON, $n = 19$), and during gamma oscillations (GAM, $n = 8$), given in arbitrary units (a.u.). Note that oxygen consumption during gamma oscillations was 2.2-fold and 5.3-fold higher as compared with spontaneous network activity and absence of spiking. Statistical significance is marked by asterisks ($P < 0.05$).

DISCUSSION

Here, we show that (1) oxygen consumption rate during gamma oscillations was 2.2-fold and 5.3-fold higher compared with spontaneous network activity and the absence of spiking, respectively. (2) Gamma oscillations as induced in the 20% O_2 gas mixture were associated with large decreases in pO_2, similar to the range observed with a hyperoxic 95% O_2 gas mixture used in previous experiments. (3) Sufficient oxygenation during fast network oscillations *in vivo* would be ensured by the computed critical radius of 30 to 40 μm around capillaries.

Gamma Oscillations in the Hippocampus and the Importance of Oxygen Supply

Gamma oscillations have been observed *in vivo* in virtually any mammalian neocortical structure and in the hippocampus.[14,15] Persistent gamma oscillations have been reliably induced *in vitro* by low concentrations of acetylcholine (carbachol) or kainic acid to activate cholinergic and glutamatergic receptors, respectively.[12,33] Such oscillations in hippocampal acute slices and slice cultures share important features with hippocampal gamma oscillations *in vivo*.[17,24] They are associated with an increase in postsynaptic potentials and action potentials; the spiking rates vary between 2 to 4 Hz and >30 Hz, depending on the type of neuron[11,34,35] (and references in ref. 13). Gamma oscillations have been observed in the presence and the absence of theta oscillations (6 to 9 Hz),[34] and the human cortex is capable to generate gamma oscillations on the time scale of minutes during mental practice.[36] Therefore, gamma oscillations *in vivo* and *in vitro* may be used as a cellular correlate for a high activity brain state.

In slice preparations, oxygen has to diffuse over greater distances into the tissue because active transport by oxygenated blood is missing. Therefore, hyperoxic conditions (95% O_2) have been used to provide oxygen in excess.[11,12] Conversely, decreased oxygen supply led to the rapid abolishment of gamma oscillations in different models and preparations from rodents, *in vitro* and *in vivo*,[11,13,33,37] perhaps because of rapid energy failure in fast-spiking inhibitory interneurons with unique electrophysiological and biochemical properties.[11,13,17] Compared with acute slices, organotypic slice cultures are thinner and have the advantage of intact cell layers on the slice cut surface because of recovery and reorganization during the culture period.[10,26] Damaged and densely packed cells are putative barriers for oxygen molecules, thus compromising oxygen supply.[38] Moreover, usage of both interface chamber and intact Biopore membrane inserts improves oxygen diffusion to the tissue, and slice cultures do not contain residual fractions of anesthetics. Thus, we show here that improved recording conditions permit investigations of persistent gamma oscillations in a gas mixture with 20% O_2, which cannot be

Table 1. Absolute values for oxygen consumption

Parameter	*Value*					*Unit*
D	*1.1*10³*	*1.3*10³*	*1.6*10³*	*1.9*10³*	*2.1*10³*	*µm²/s*
A for TTX	13.9	16.4	20.3	24.1	26.4	mm Hg/s
	1.42	1.68	2.08	2.45	2.71	mmol/L per minute
A for SPON	30.7	35.5	44.7	53.0	58.7	mm Hg/s
	3.14	3.64	4.59	5.44	6.02	mmol/L per minute
A for GAM	75.8	89.3	107.3	121.8	140.9	mm Hg/s
	7.77	9.12	11.01	12.46	14.46	mmol/L per minute

The absolute values for oxygen consumption (*A*) were calculated with various diffusion coefficients (*D*) for the three different activity states of the hippocampal CA3 network, i.e., absence of spiking (TTX), spontaneous network activity (SPON), and gamma oscillations (GAM). The values are provided in units, mm Hg/s, and mmol/L per minute.

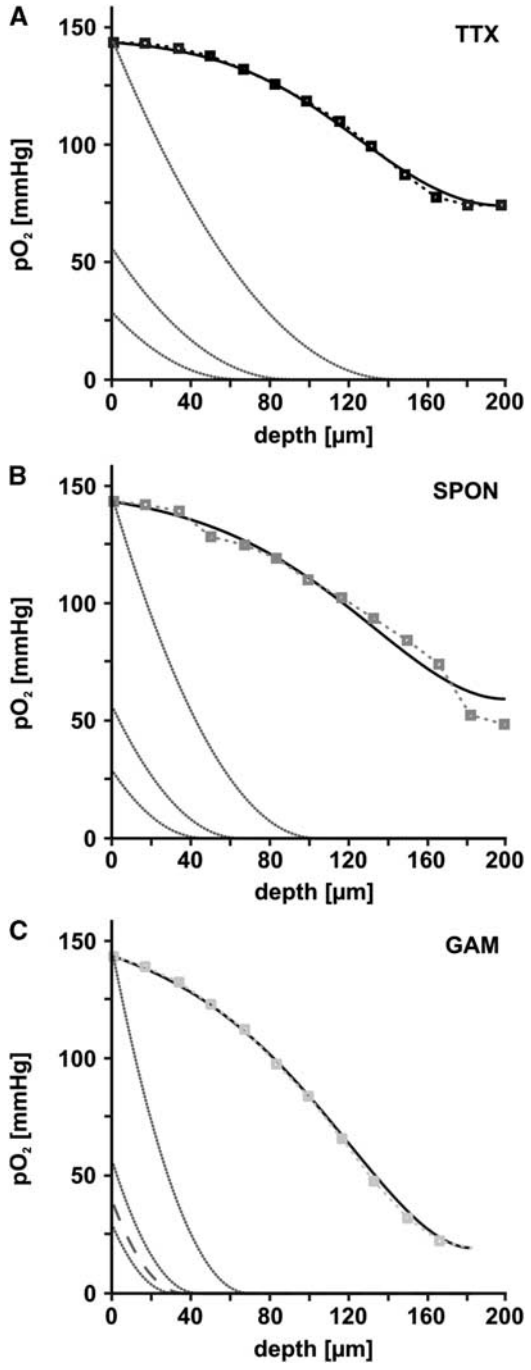

Figure 5. Application of the model to estimate *in vivo* conditions. Experimentally determined values (small boxes) and simulated partial oxygen pressure (pO_2) depth profiles for the three different activity states, i.e., tetrodotoxin (TTX) (**A**), spontaneous network activity (SPON) (**B**), and gamma oscillations (GAM) (**C**), are shown by black lines (see also Figures 4A to 4C). In each panel, the first dark gray line illustrates the simulated pO_2 depth profile assuming that the convective component was absent and oxygen consumption was unaltered. When applying physiologic boundary conditions of 55 mm Hg (second dark gray line) or 28 mm Hg (third dark gray line) and again fixing the oxygen consumption to the same value, the resulting simulated pO_2 profiles reveal the radius around a vessel, in which neuronal tissue is sufficiently supplied with oxygen. In (**C**), the broken line depicts the pO_2 profile with the lowest oxygen boundary condition ($\sim$40 mm Hg) that is still capable to fuel gamma oscillations at a distance of $\sim$35 μm midway between capillaries. Lower oxygen boundary conditions would require a hemodynamic response to maintain gamma oscillations.

achieved under (semi)submerged recording conditions.[11,13] Moreover, we show that decreases in pO_2 during gamma oscillations were similar compared with the gas mixture of 95% O_2 (ref. 17), suggesting that respiratory uncoupling in hyperoxic slice layers[39] is not a crucial factor for high oxygen consumption rate during gamma oscillations. However, decreases in pO_2 might reflect both activity-dependent oxygen consumption and limitation of oxygen transport into the slice. To take both processes into account, we developed a mathematical model to obtain a relative quantification of oxygen consumption rate during spontaneous network activity and gamma oscillations.

Quantification of O_2 Consumption Rates by Mathematical Modeling

We established a reaction-diffusion model to quantify the oxygen consumption rates in slice cultures during three well-defined activity states in hippocampal area CA3. Since all pO_2 profiles showed convex characteristics in the upper part of the slice, we included an exponentially declining convective oxygen transport (decay length $\sim$40 μm), in addition to diffusive oxygen supply. To our knowledge, an initial convex part of the pO_2 depth profiles has never been reported, likely because of usage of thicker brain slices (1 to 1.5 mm) and lower spatial resolution (step sizes of $\sim$100 μm). However, the convex part might be appreciated in illustrated pO_2 profiles from earlier studies.[27,28] By means of the mathematical model, we were able to quantify the oxygen consumption rates during gamma oscillations (GAM) in relation to spontaneous network activity (SPON) and the absence of spiking (TTX). The TTX blocks fast voltage-gated Na^+ channels and thus suppresses the generation of action potentials in neuronal tissue. However, TTX leaves several other neuronal processes widely unaffected such as maintenance of resting membrane potentials and quantal release of neurotransmitters, with subsequent occurrence of miniature postsynaptic potentials. Thus, the TTX condition provides a good model for a widely inactive neuronal network. By contrast, hippocampal gamma oscillations *in vitro* may represent a high activity brain state and primarily reflect averaged synchronized inhibitory postsynaptic potentials in the perisomatic region rather than action potentials and excitatory postsynaptic potentials.[12,14] Our experimental data and calculations suggest that gamma oscillations are associated with 2.2-fold and 5.3-fold higher oxygen consumption rate compared with spontaneous network activity and absence of spiking, respectively. Therefore, we conclude that the maximal variation of local oxygen consumption rate in brain tissue is in the order of a factor of about five.

Implications for Oxygen Consumption and Vasculature System *In Vivo*

As the reference condition, we suppressed spiking in slice cultures by TTX, notably in the absence of any anesthetics. This differs to a certain degree from pO_2 measurements in anesthetized animals because anesthetics have been reported to significantly interfere with both neuronal activity and energy metabolism.[24,25] However, recently it was shown in anesthetized rats that local oxygen consumption was significantly increased by all aspects of neuronal signaling, i.e., spontaneous and stimulus-induced Purkinje cell spiking and postsynaptic processes in the cerebellar cortex, while a large fraction of basal oxygen consumption was left intact in the presence of TTX (ref. 6). The state of spontaneous network activity in slice cultures may correspond to a brain state where spiking is not suppressed but external afferent input such as optical or visual stimulation is lacking. Spontaneous network activity is variable in slice cultures,[13,16] which might correspond to spontaneous fluctuations in the blood oxygen level-dependent signal, observed even in the absence of explicit input or output.[40] Finally, gamma oscillations in slice cultures may represent a high activity brain state that is associated with higher cognitive

functions, such as sensory processing, memory formation, and attentional selection.[14,15] However, it is important to note that gamma oscillations of high amplitude are generated in the rodent hippocampal CA3 area; and recent evidence suggests that neuronal mitochondria in this area show specific enzymatic properties to match the high energy demand associated with gamma oscillations.[17] Such unique electrophysiological and biochemical features may not necessarily apply to other cortical regions expressing gamma oscillations.[15] However, our estimates of the relative increase in oxygen consumption rates during different activity states in slice cultures are in good agreement with recent *in vivo* data, according to which the basal energy utilization of the deeply anesthetized brain is $\sim$20% of the conscious brain and that at the threshold of loss of consciousness, the energy utilization decreases by 40% to 50% (ref. 41).

In vivo, oxygen availability is dependent on active transport processes through blood vessels and passive oxygen diffusion through brain tissue. Enhanced neuronal activity is associated with a local rise in blood flow within a few seconds that markedly increases oxygenation at the capillary level.[4,5,18] From the capillary, oxygen has to diffuse into the brain parenchyma. Tissue oxygenation by sole oxygen diffusion was mimicked by model simulations where the convective oxygen transport was put to zero and the pO_2 at the interphase between the capillary and the tissue was varied between 55 and 28 mm Hg.[19,31] The obtained pO_2 profile suggests that sufficient oxygenation of brain tissue during gamma oscillations is only possible in a radius of $\sim$30 to 40 μm from the capillary, which is in line with distances of 40 to 70 μm between capillaries in men and rodents.[19,21,32,42] Thus, we conclude that the effort spent on the structure of the vasculature system is economized to just match the energy demand that is associated with high activity states such as gamma oscillations. Conversely, higher intercapillary distances might not permit prolonged periods of gamma oscillations,[36] unless compensatory hemodynamic responses occur.[7,43] This notion is substantiated by observations that a strong geometrical association exists between vasculature and tissue oxygen availability[19] and that under chronic hypoxic conditions the intercapillary distance shortens because of enhanced angiogenesis.[44]

DISCLOSURE/CONFLICT OF INTEREST

The authors declare no conflict of interest.

ACKNOWLEDGEMENTS

The authors thank Andrea Lewen and Dr Uwe Heinemann for technical support and valuable discussion.

REFERENCES

1 Erecińska M, Silver IA. Tissue oxygen tension and brain sensitivity to hypoxia. *Respir Physiol* 2001; **128**: 263–276.
2 Fox PT, Raichle ME, Mintun MA, Dence C. Nonoxidative glucose consumption during focal physiologic neural activity. *Science* 1988; **241**: 462–464.
3 Shulman RG, Hyder F, Rothman DL. Lactate efflux and the neuroenergetic basis of brain function. *NMR Biomed* 2001; **14**: 389–396.
4 Buxton RB. Interpreting oxygenation-based neuroimaging signals: the importance and the challenge of understanding brain oxygen metabolism. *Front Neuroenergetics* 2010; **2**: 8.
5 Masamoto K, Omura T, Takizawa N, Kobayashi H, Katura T, Maki A *et al.* Biphasic changes in tissue partial pressure of oxygen closely related to localized neural activity in guinea pig auditory cortex. *J Cereb Blood Flow Metab* 2003; **23**: 1075–1084.
6 Thomsen K, Piilgaard H, Gjedde A, Bonvento G, Lauritzen M. Principal cell spiking, postsynaptic excitation, and oxygen consumption in the rat cerebellar cortex. *J Neurophysiol* 2009; **102**: 1503–1512.
7 Devor A, Sakadžić S, Saisan PA, Yaseen MA, Roussakis E, Srinivasan VJ *et al.* 'Overshoot' of O_2 is required to maintain baseline tissue oxygenation at locations distal to blood vessels. *J Neurosci* 2011; **31**: 13676–13681.
8 Kim S-G, Uğurbil K. Comparison of blood oxygenation and cerebral blood flow effects in fMRI: estimation of relative oxygen consumption change. *Magn Reson Med* 1997; **38**: 59–65.
9 Okada Y, Lipton P. Glucose, oxidative energy metabolism, and neural function in brain slices—glycolysis plays a key role in neural activity. In: Lajtha A, Gibson GE, Dienel GA (eds). *Handbook of Neurochemistry and Molecular Neurobiology. Brain Energetics. Integration of Molecular and Cellular Processes*. Springer: Berlin-Heidelberg, 2007, pp 17–39.
10 Kann O, Kovács R. Mitochondria and neuronal activity. *Am J Physiol Cell Physiol* 2007; **292**: C641–C657.
11 Hájos N, Ellender TJ, Zemankovics R, Mann EO, Exley R, Cragg SJ *et al.* Maintaining network activity in submerged hippocampal slices: importance of oxygen supply. *Eur J Neurosci* 2009; **29**: 319–327.
12 Fisahn A, Pike FG, Buhl EH, Paulsen O. Cholinergic induction of network oscillations at 40 Hz in the hippocampus *in vitro*. *Nature* 1998; **394**: 186–189.
13 Huchzermeyer C, Albus K, Gabriel H-J, Otáhal J, Taubenberger N, Heinemann U *et al.* Gamma oscillations and spontaneous network activity in the hippocampus are highly sensitive to decreases in pO_2 and concomitant changes in mitochondrial redox state. *J Neurosci* 2008; **28**: 1153–1162.
14 Bartos M, Vida I, Jonas P. Synaptic mechanisms of synchronized gamma oscillations in inhibitory interneuron networks. *Nat Rev Neurosci* 2007; **8**: 45–56.
15 Uhlhaas PJ, Singer W. Abnormal neural oscillations and synchrony in schizophrenia. *Nat Rev Neurosci* 2010; **11**: 100–113.
16 Sasaki T, Matsuki N, Ikegaya Y. Metastability of active CA3 networks. *J Neurosci* 2007; **27**: 517–528.
17 Kann O, Huchzermeyer C, Kovács R, Wirtz S, Schuelke M. Gamma oscillations in the hippocampus require high complex I gene expression and strong functional performance of mitochondria. *Brain* 2011; **134**: 345–358.
18 Offenhauser N, Thomsen K, Caesar K, Lauritzen M. Activity-induced tissue oxygenation changes in rat cerebellar cortex: interplay of postsynaptic activation and blood flow. *J Physiol* 2005; **565**: 279–294.
19 Kasischke KA, Lambert EM, Panepento B, Sun A, Gelbard HA, Burgess RW *et al.* Two-photon NADH imaging exposes boundaries of oxygen diffusion in cortical vascular supply regions. *J Cereb Blood Flow Metab* 2011; **31**: 68–81.
20 McGoron AJ, Nair P, Schubert RW. Michaelis-Menten kinetics model of oxygen consumption by rat brain slices following hypoxia. *Ann Biomed Eng* 1997; **25**: 565–572.
21 Thews G. Die Sauerstoffdiffusion im Gehirn (Oxygen diffusion in brain). *Pflugers Arch* 1960; **271**: 197–226.
22 Evans NTS, Naylor PFD, Quinton TH. The diffusion coefficient of oxygen in respiring kidney and tumour tissue. *Respir Physiol* 1981; **43**: 179–188.
23 Homer LD, Shelton JB, Williams TJ. Diffusion of oxygen in slices of rat brain. *Am J Physiol* 1983; **244**: R15–R22.
24 Whittington MA, Faulkner HJ, Doheny HC, Traub RD. Neuronal fast oscillations as a target site for psychoactive drugs. *Pharmacol Ther* 2000; **86**: 171–190.
25 Muravchick S, Levy RJ. Clinical implications of mitochondrial dysfunction. *Anesthesiology* 2006; **105**: 819–837.
26 Bahr BA, Kessler M, Rivera S, Vanderklish PW, Hall RA, Mutneja MS *et al.* Stable maintenance of glutamate receptors and other synaptic components in long-term hippocampal slices. *Hippocampus* 1995; **5**: 425–439.
27 Jiang C, Agulian S, Haddad GG. O_2 tension in adult and neonatal brain slices under several experimental conditions. *Brain Res* 1991; **568**: 159–164.
28 Brockhaus J, Ballanyi K, Smith JC, Richter DW. Microenvironment of respiratory neurons in the *in vitro* brainstem-spinal cord of neonatal rats. *J Physiol* 1993; **462**: 421–445.
29 Hall CN, Klein-Flügge MC, Howarth C, Attwell D. Oxidative phosphorylation, not glycolysis, powers presynaptic and postsynaptic mechanisms underlying brain information processing. *J Neurosci* 2012; **32**: 8940–8951.
30 Sokoloff L, Reivich M, Kennedy C, Des Rosiers MH, Patlak CS, Pettigrew KD *et al.* The [^{14}C]deoxyglucose method for the measurement of local cerebral glucose utilization: theory, procedure, and normal values in the conscious and anesthetized albino rat. *J Neurochem* 1977; **28**: 897–916.
31 Vovenko E. Distribution of oxygen tension on the surface of arterioles, capillaries and venules of brain cortex and in tissue in normoxia: an experimental study on rats. *Pflugers Arch* 1999; **437**: 617–623.
32 Tata DA, Anderson BJ. A new method for the investigation of capillary structure. *J Neurosci Methods* 2002; **113**: 199–206.
33 Fano S, Behrens CJ, Heinemann U. Hypoxia suppresses kainate-induced γ-oscillations in rat hippocampal slices. *NeuroReport* 2007; **18**: 1827–1831.
34 Buzsáki G, Buhl DL, Harris KD, Csicsvari J, Czéh B, Morozov A. Hippocampal network patterns of activity in the mouse. *Neuroscience* 2003; **116**: 201–211.
35 Dugladze T, Schmitz D, Whittington MA, Vida I, Gloveli T. Segregation of axonal and somatic activity during fast network oscillations. *Science* 2012; **336**: 1458–1461.
36 Lutz A, Greischar LL, Rawlings NB, Ricard M, Davidson RJ. Long-term meditators self-induce high-amplitude gamma synchrony during mental practice. *Proc Natl Acad Sci USA* 2004; **101**: 16369–16373.

37 Barth AMI, Mody I. Changes in hippocampal neuronal activity during and after unilateral selective hippocampal ischemia *in vivo*. *J Neurosci* 2011; **31**: 851–860.
38 Hu HP, Wu MX. Mechanism of anesthetic action: oxygen pathway perturbation hypothesis. *Med Hypotheses* 2001; **57**: 619–627.
39 Andrews ZB, Diano S, Horvath TL. Mitochondrial uncoupling proteins in the CNS: in support of function and survival. *Nat Rev Neurosci* 2005; **6**: 829–840.
40 Fox MD, Raichle ME. Spontaneous fluctuations in brain activity observed with functional magnetic resonance imaging. *Nat Rev Neurosci* 2007; **8**: 700–711.
41 Shulman RG, Hyder F, Rothman DL. Baseline brain energy supports the state of consciousness. *Proc Natl Acad Sci USA* 2009; **106**: 11096–11101.
42 Meier-Ruge W, Ulrich J, Stähelin HB. Morphometric investigation of nerve cells, neuropil and senile plaques in senile dementia of the Alzheimer type. *Arch Gerontol Geriatr* 1985; **4**: 219–229.
43 Niessing J, Ebisch B, Schmidt KE, Niessing M, Singer W, Galuske RAW. Hemodynamic signals correlate tightly with synchronized gamma oscillations. *Science* 2005; **309**: 948–951.
44 LaManna JC, Chavez JC, Pichiule P. Structural and functional adaptation to hypoxia in the rat brain. *J Exp Biol* 2004; **207**: 3163–3169.

Supplementary Information accompanies the paper on the Journal of Cerebral Blood Flow & Metabolism website (http://www.nature.com/jcbfm)